2018

Vehicle-to-barrier communication during real-world vehicle crash tests

Samil Temel

Mehmet C. Vuran

Mohammad M.R. Lunar

Zhongyuan Zhao

Abdul Salam

See next page for additional authors

Authors
Samil Temel, Mehmet C. Vuran, Mohammad M.R. Lunar, Zhongyuan Zhao, Abdul Salam, Ronald K. Faller, and Cody S. Stolle

Vehicle-to-barrier communication during real-world vehicle crash tests

Samil Temel,[1] Mehmet C. Vuran,[2]
Mohammad M.R. Lunar,[2] Zhongyuan Zhao,[2]
Abdul Salam,[2] Ronald K. Faller,[3] & Cody Stolle[3]

1 Turkish Air Force, Izmir, Turkey
2 Cyber-physical Networking Laboratory, Computer Science and Engineering, University of Nebraska-Lincoln, Lincoln, NE, USA
3 Midwest Roadside Safety Facility, University of Nebraska-Lincoln, Lincoln, NE, USA

Corresponding author — M.M.R. Lunar, *email* mlunar@cse.unl.edu

E-mail addresses — stemel@unl.edu (S. Temel), mcvuran@cse.unl.edu (M.C. Vuran), mlunar@cse.unl.edu (M.M.R. Lunar), zhzhao@cse.unl.edu (Z. Zhao), asalam@cse.unl.edu (A. Salam), rfaller1@unl.edu (R.K. Faller), cstolle2@unl.edu (C. Stolle).

Abstract

Vehicle-to-barrier (V2B) communication is expected to facilitate wireless interactions between vehicles and roadside barriers in next-generation intelligent transportation systems. V2B systems will help mitigate single-vehicle, run-off-road crashes, which account for more than 50% of roadside crash fatalities. In this work, the characteristics of the wireless channel prior to and during a crash are analyzed using orthogonal frequency division multiplexing (OFDM) techniques, which has been used in existing vehicular communication systems. More specifically, the performance of OFDM-based V2B links are measured in real-world crash tests for the

Published in *Computer Communications* 127 (2018), pp 172–186.
doi 10.1016/j.comcom.2018.05.009

Submitted 1 May 2017; revised 9 May 2018; accepted 18 May 2018; published 26 May 2018.

first time. Three crash tests conducted at the Midwest Roadside Safety Facility, Lincoln, Nebraska, are reported: a bogie vehicle crashing into a soil-embedded post at 27 mph, a sedan crashing to a concrete curb at 15 mph, and a pickup crashing to a steel barrier at 62 mph. Metrics including signal to interference plus noise ratio received signal strength, error vector magnitude, phase error, channel coherence, and bit error rate, are used to illustrate the impacts of antenna type, antenna deployment, speed, and mobility during the crash tests. The empirical evidence shows that barrier-height (0.7–0.9 m) antennas at the barrier can improve V2B signal quality compared to higher deployments (≥1.5 m) due to the stronger reflection of electromagnetic waves at a larger angle of incidence. Moreover, compared to omni-directional barrier antennas, directional barrier antennas can increase signal quality, connectivity, and coherence time of V2B channel because of reduced multi-path effects, however, the antenna orientation needs to be carefully determined to maintain connectivity.

Keywords: Vehicle-to-barrier communications, Vehicle crash, OFDM impairments

1. Introduction

Connected vehicles of tomorrow and autonomous vehicles of the near future are slated to operate on roadside infrastructure designed decades ago. Today, more than 50% of all traffic fatalities are a result of run-off-road (RoR) crashes [1–3]. These RoR crashes include vehicular crashes caused by hitting the fixed objects, rollovers, cross-median crashes, return-to-travelway crashes etc. Specifically, 40% of the defined RoR crashes represents single-vehicle crashes [2]. Roughly 20% of all traffic fatalities are related to RoR fixed-object crashes [4]. Recent vehicles are equipped with sensory technologies, such as blind-spot detection or lane-departure warning. Yet, recent statistics released by the White House and U.S. Department of Transportation's National Highway Traffic Safety Administration show that 8.3% (2,483) more people died in traffic-related accidents in 2015 than in 2014, and this increasing trend continued in 2016 with 5.8% (1900) more fatalities compared to 2015 [5]. This unfortunate data point breaks a recent historical trend of fewer deaths occurring per year [6].

For nearly two decades, intelligent transportation systems (ITS) have been in development to provide transportation systems with information and communication facilities. New technologies are developed for connected vehicles dubbed V2X communication paradigms (**Fig. 1**): such as vehicle-to-vehicle (V2V) [8], vehicle-to-infrastructure (V2I) [9], vehicle-to-pedestrian (V2P) [10], and vehicle-to-cloud (V2C) [11]. The recent ITS strategic plan aims to

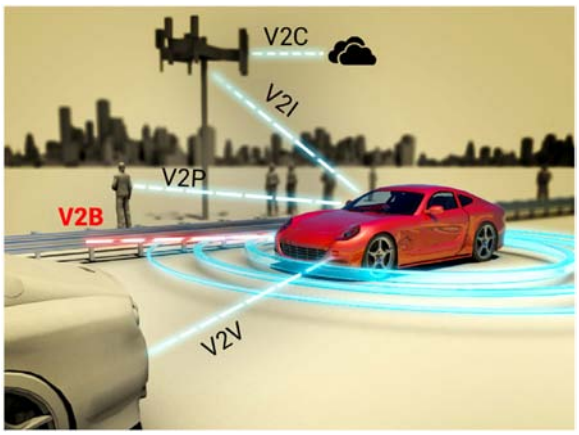

Fig. 1. Vehicular communication technologies [7].

enable safer vehicles and safer roadways by developing better crash avoidance for all road vehicles [12]. The available intelligent collision avoidance mechanisms mostly focus on inter-vehicle collisions [13–15].

2. Motivation and V2B use cases

The core motivation of V2B communications is to prevent and mitigate run-off-road crashes. A car-to-barrier crash lasts nearly 1 to 2 seconds; depending on the encroachment velocity of the vehicle [16]. Introduction of a V2B communication infrastructure that shares information between errant vehicles and roadside barriers will lead to a rapid-response safety system, detect an on-coming crash, take precautions within vehicle to avoid the crash, and if a crash is inevitable, take control of vehicle to mitigate severe impacts.

We believe the development of V2B systems will complement existing V2X technologies by focusing on safety issues related to single-vehicle RoR fatalities and serious injuries. By enhancing communication capabilities between the vehicles and roadside barriers, V2B systems would not only augment the automation technologies but also present robust solutions to keep vehicles safe on the roads. In this regard, *Vehicle-to-barrier (V2B) communications* is introduced as an additional tool for the V2X paradigm. The motivation for V2B and comparisons to existing V2X technologies in terms of functionalities and characteristics are further discussed in the following. We also discuss potential operational aspects of V2B systems that will be enabled by V2B communications.

2.1. Motivation

RoR crash prevention/mitigation: Currently, most active safety systems solely rely on on-board sensors, such as camera, ultrasonic and/ or Laser sensors. However, in the case of on-board sensory failures, fatal accidents could occur. The most prominent example is the recent fatal crash of a commercial electric car on autopilot to a highway barrier, killing its driver [17]. As the auto manufacturer stated, "Autopilot does not prevent all accidents." Similarly, there is no support to prevent *all* run-off-road crashes in existing technologies including IEEE 802.11p, dedicated short range communications (DSRC), and LTE. These communication architectures are primarily designed to ensure communications and are mostly installed in urban and populated areas [18,19]. For example, DSRC Crash Avoidance Safety application relies on MapData (MAP), and Signal Phase and Timing (SPaT) to prevent vehicle to vehicle crashes. The required data is only available at the intersections. Moreover, recent V2V technologies alone, cannot address single-car crashes, which account for more than 50% of fatalities.

It is clear that relying only on on-board sensors, inter-vehicle communication, or roadside units on urban intersections cannot prevent all RoR crashes. To this end, the recent improvements in low-cost wireless communication technologies allow for a new kind of V2X communication, V2B, to connect vehicles with barriers. Typical environments of the vehicular infrastructures are highways, urban, suburban and rural areas, in tunnels, or on bridges [20–22]. V2B solutions, when deployed efficiently at these hot-spot locations, can complement existing safety technologies. To help prevent run-off-road crashes, V2B links can communicate information about the existence of roadside infrastructure, e.g., barriers; as well as its properties, e.g., road type, shoulder type, barrier type, barrier location. Yet, V2B communications is unique due to high speeds involved, dynamically reducing distances, and different deployment opportunities due to the existing barriers and their different types. Therefore, there is a need to conduct wireless communication evaluations in *car crash scenarios* in these environments.

Latency: Given the 1–2 s interval during a crash, establishing communication between an errant vehicle and a barrier radio within sub-second delay is important for the parties to exchange relevant information (vehicle speed, barrier type, barrier location, road and shoulder type, etc.), detect that a crash may be imminent, request further information from the barrier for control decisions, alert the driver, and/or take control of the car to avoid or mitigate the crash. This tight delay requirement may limit the applicability of existing V2X solutions and standards to V2B systems. The main emphasis of existing V2I systems is on improving network capacity [23], therefore V2I systems are mainly designed for content delivery and are inherently tolerant to latency [24]. For example, IEEE 802.11p standard incorporates

delays in the range of 1–2 s to activate a link and associate with a roadside unit (RSU) [24–27]. Moreover, even though an emergency channel is allocated, the broadcast nature of DSRC communications leads to channel congestion and spectrum sharing issues in the 5.9 GHz DSRC band (safety channel 172) [28]. Since sharing the single emergency channel for both V2V and V2B communication is challenging, the existing standard may not be feasible for time-sensitive run-off-road crashes prevention. Cellular technologies also suffer from high latency [29]. For example, LTE for vehicular applications is limited to latencies of 1–2 s [30], which constitute the motivation for new 5G technologies. Therefore, providing a V2B communication infrastructure between errant vehicles and roadside barriers, for a *rapid-response* safety system that reacts in orders of a few hundred milliseconds, may not be feasible with existing standards, which need to be augmented or extended to support V2B system requirements.

Connectivity: There are other limitations in IEEE 802.11p, dedicated short range communications (DSRC), and V2B is designed to overcome these limitations. For example, with IEEE 802.11p and DSRC, coverage cannot be guaranteed for all vehicles on the road because of the deployment density [19]. All vehicles cannot receive the same performance due to the weak signals at the receiver. Not every vehicle could have a reliable connectivity due to channel fading. Time to establish the connection is a limiting factor in existing technologies for their application to run-off-road crashes the due to overhead at the higher layers.

High mobility and speeds: Traditional vehicular communication technologies are characterized by high mobility and various types of environments [20]. The velocity of nodes in real-world vehicular experiments, usually range from 22–77 mph (9.8–34.4 m/s) [31,32]. High velocities of nodes in vehicular networks place significant challenges on designing wireless communication solutions. Field test shows that vehicle speed affects operating performance of IEEE 802.11p-like systems [32]. Yet, in most V2V scenarios, the *relative* speed between radios is much smaller because the vehicles travel at similar speeds. For V2B communications, we are interested in communication between an errant vehicle and a *stationary* barrier, where the relative speed between radios is similar to the vehicle speed *and* the distance between two radios decreases rapidly. For vehicular communication systems based on orthogonal frequency division multiplexing (OFDM) techniques, channel variations within a few OFDM symbols would cause inter-symbol interference (ISI), which is especially detrimental for future V2B systems in car crash scenarios. Understanding the V2B channel, especially during a RoR crash, would serve valuable insights for the design of reliable and robust V2B solutions. One of the most prominent factors on vehicular communication impairments is the Doppler spread [33]. Doppler shift causes a mismatch between frequencies of the received signal and local oscillator,

which destroys the orthogonality of the sub-carriers during an OFDM transmission. For OFDM systems with high mobility, the carrier frequency offset (CFO) and Doppler shift cause inter-carrier interference (ICI) [34]. These signal impairments can be observed through various performance metrics, such as received signal strength (RSS), peak-to-average power ratio (PAPR), error vector magnitude (EVM), and phase error (PE) [35,36], which are of interest in this paper.

Deployment height: The existing V2I systems are mostly installed in urban areas, where roadside infrastructures are available. In almost all these cases, the V2I infrastructures are much higher as compared to traditional roadside barriers [37]. On the other hand, we show that V2B communications may benefit from a barrier-height deployment [7]. There is a significant improvement on signal strength when the receiver antennas are deployed on lower heights (0.82m - barrier height and 1.4m - roof-top of a sedan car height) than higher ones (1.9m - rooftop of an SUV car and 3m - traffic signal height). Moreover, during a vehicle brake, a 3m receiver antenna exhibited the worse results regarding signal impairments. Thus, for V2B systems, we mainly project deployment of antennas on or close to the height of generally used barriers. Moreover, there is a need to develop signal transmission methods and algorithms which exploit the reception of higher signal strengths and minimize the effect of signal impairments during a transmission. Yet, existing studies have either not considered V2B communications or are limited to drive-by experiments.

2.2. V2B use cases

RoR crash avoidance: The established link between the vehicle and the barrier can exchange information including current position and direction of the car, current weather condition, current road condition. By using this information the V2B system can prepare a safety critical warning for the driver of the car is he/she approaches towards a barrier for a prospective crash. In addition to the main objective of crash avoidance, V2B communications can also lead to several novel applications, a few of which are discussed below.

Replacement of physical barriers with virtual barriers: With the advancement of V2B technology, it is also possible to replace the physical barrier system with a virtual barrier system. A virtual barrier can transmit beacons to approaching vehicles such that necessary control actions can be taken by on-board active safety systems. The objective of physical barriers is to prevent vehicle running off the road and falling in hazardous zones. However, the physical barrier itself can be dangerous for passengers. Proper deployment of the virtual barrier systems could make existing barriers less destructive.

Relative positioning: Even though existing ITS solutions rely heavily on GPS, which provides an accurate information about the location of a vehicle with respect to the Earth, locating a vehicle with respect to the roadside infrastructure is still challenging due to lack of information about roads. An array of synchronized barriers can provide positioning capabilities for the vehicles. The vehicle can position itself through a radio-based localization solution, e.g., time differences of arrival (TDoA) of timestamped beacon packets transmitted from barriers and/or RSS-based fingerprinting [38]. Alternatively, connected barriers can also position a vehicle by measuring the TDoA and/or RSS of packets transmitted from the vehicle. With connected barriers, runoff- road situations could be detected by either the vehicle or infrastructure, and critical safety signal can be issued to the on-board active and passive safety systems of the errant vehicle hundreds of milliseconds before the accident.

Based on the aforementioned motivations, the main focus of this paper is the characterization of the V2B channel during a crash to analyze impacts of speed, antenna location, antenna type, and crash type. More specifically, we present evaluation results of OFDM-based V2B communication experiment in three real-world crash tests conducted at the outdoor proving grounds of Midwest Roadside Safety Facility (MwRSF), Lincoln, Nebraska, in 2016–2017.[1] The first test is a bogie vehicle crash to a soil-embedded post at 27 mph (June 2016). The second test is a Toyota sedan crash to a concrete curb at 15 mph (June 2016). The third test is a pickup crash to steel barrier at 62 mph (November 2017). We present the OFDM signal impairment results for average received signal strength (RSS), signal to interference and noise ratio (SINR), error vector magnitude (EVM) and phase error (PE), Bit Error Rate (BER), burst errors, and channel coherence. To the best of our knowledge, this is the first study that evaluates wireless communication during real-world crash tests.

The rest of this paper is organized as follows: The experimental setups and data analyzing approaches are introduced in Section 3. In Section 4, key test results are presented and discussed. Finally, the paper is concluded in Section 5.

3. Experimental setup

The wireless communication experiments are piggybacked on four crash tests at MwRSF:

Bogie to post crash (bogie) test: In this test, a bogie vehicle, as shown in Fig. 3(a), is crashed into a post buried in the ground. The experimental setup is

1 An earlier version of this paper appeared in IEEE VNC 2016 [39].

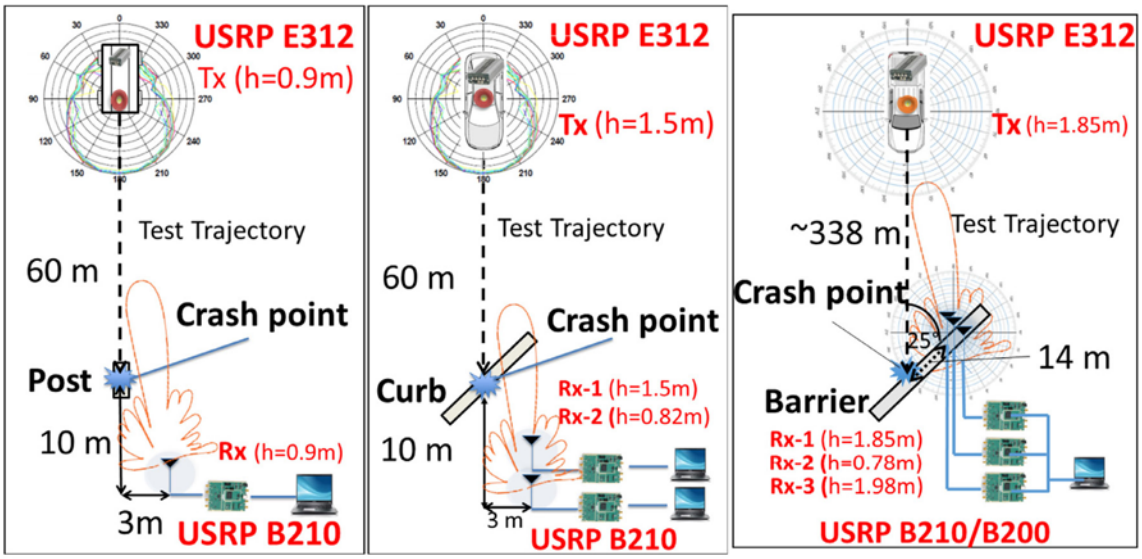

(a) Bogie to Post (b) Sedan to Curb (c) Pickup to Steel Barrier

Fig. 2. Crash test setup [40,41].

illustrated in Fig. 2(a). The bogie started its journey 60 m away from the crash point, and crashed to the post with a velocity of 27 mph (12.1 m/s). Snapshots from the experiment at the beginning, encroachment, crash, and post-crash are shown in Fig. 6(a)–(d). This test is referred as bogie test in the paper.

Sedan to curb crash (sedan) test : In this test, a sedan car, as shown in Fig. 4(a), is crashed into a curb. The experimental setup is illustrated in Fig. 2(b). The test sedan started its journey 60 m away from the impact point, and crashed to the curb at an angle of 40° with a velocity of 15 mph (6.7 m/s). Snapshots from the experiments at the beginning, crash, and post-crash are shown in Fig. 6(e)–(g). This test is referred as sedan test in the paper.

Pickup to steel barrier crash (pickup) test: In this test, a pickup truck as shown in Fig. 5, is crashed into a 0.78m high steel barrier. Fig. 2(c) explains the test plan of this crash test. Initially, the sedan is placed around 338 m away from the impact point. It is then crashed to the barrier at an angle of 25° with a velocity of 62 mph (27.7 m/s). Snapshots of this crash test is shown in Fig. 6(h)–(j). This test is referred as pickup test in the paper.

Bogie test is a well-accepted low-cost approach for real-world crash tests in roadside safety community. Therefore, it is important to analyze similarities of V2B communication in such settings so that more controlled crash experiments can be conducted with bogie while still collecting important relevant data. Although the height and width of bogie is 40% and 10% smaller than the sedan used in sedan test, their mobility patterns are designed to be similar in crash scenarios. As shown in Section 4.1, the smaller height and size of bogie lead to shorter shadow fading distances (about 25%), however,

(a) Bogie

(b) Vehicle (left) and barrier (right) antennas

Fig. 3. Bogie test devices

(a) vehicle and curb (b) Vehicle(left) Rx(right) Antennas

Fig. 4. Sedan test devices.

(a) Vehicle Antenna (b) Barrier Antennas

Fig. 5. Pickup test devices.

Fig. 6. Snapshots of different stages of crash tests: (a–d) Bogie, (e–g) Sedan, and (h–j) Pickup.

such influence persists throughout the test. In contrast, as shown in Section 4.4, the impairments on vehicle to barrier communication are observed on bogie, sedan, and pickup tests since such impairments are mostly contributed by the mobility pattern during the crash.

It can be observed in Fig. 6 that the environments of the three tests are different reflecting different roadside conditions. The bogie test (Fig. 6(a)–(d)) is conducted in an open ground with only a few humans, objects, and no buildings, while the location of sedan test (Fig. 6(e)–(g)) is surrounded by several buildings, mechanical equipment, and there are a number of personals and vehicles during the experiment. The pickup test (Fig. 6(h)–(j)) is also conducted in an open ground similar to the bogie test. However, it was surrounded by some concrete and steel barriers for stopping the pickup truck after the crash, and several big mechanical equipment. In these crash tests, the test vehicle is accelerated by another cable-connected vehicle, and released shortly before the crash. Communication experiments are conducted during the crash tests. Next, we introduce the experiment setup followed by data processing and performance metrics.

3.1. V2B communication experiment setup

OFDM-based wireless communication at 5.8 GHz is conducted from a transmitter (vehicle antenna) mounted on the test vehicle, to one or multiple receivers (barrier antenna) placed at a safe location behind the impact point (post, curb, and barrier). The transmitter is implemented with a battery-powered USRP E312, which integrates an Ubuntu operating system-based embedded controller, motion sensors, and a GPS receiver. The receivers are implemented with a USRP B210 connected to a laptop computer. When multiple receivers are used, their time is synchronized over the Internet with NTP in advance. GNU Radio-based OFDM benchmark codes [43] are used at the transmitter and receiver. Raw IQ data recorded by the receiver is stored in the host computer and processed off-line.

V2B communications are expected to be bi-directional to inform a vehicle about barrier and road conditions ($V \rightarrow B$) and request additional information from the barrier in case an imminent crash is detected ($B \rightarrow V$). The communication direction during the experiments is selected to be from the vehicle to barrier because of mainly practical considerations. Since an embedded radio is used in the crash, its processing and storage capabilities are limited. Therefore, vehicle radios are used for transmission. Moreover, there are concerns of data loss in case the crash damages the vehicle radio. Since the crash experiments are highly expensive and cannot be repeated on demand, this selection ensures the safety of the data, which is collected at the barrier radios. Moreover, the experiments are conducted on line-of-sight environments. Therefore, $V \rightarrow B$ experiments are representative of $B \rightarrow V$ direction due to channel symmetry.

Key technical specifications of the antennas used in the experiments are listed in Table 1. In bogie and sedan tests, the vehicle is equipped with a mini panel antenna, and the barrier is equipped with a panel antenna mounted on a tripod, as shown in Figs. 3(b) and 4(b). The mini panel, and the panel antennas are both directional. For pickup test, the vehicle antenna is omni-directional, and barrier radios are equipped with either omni-directional or directional antennas, as shown in Fig. 5(a).

In bogie test, the vehicle antenna is mounted 1 m behind the front bumper of the bogie at a height of 0.90 m (Fig. 3(b)). The barrier antenna is installed 10 m behind the crash impact point with a height of 0.90 m (Fig. 3(b)).

Table 1. Antenna specification in crash tests.

Deployment	*Type*	*Gain*	*Beam-width (horizontal/vertical)*
Vehicle (Tx)	Mini panel	10 dBi	16°/66° [40]
Barrier (Rx)	Panel	23 dBi	12°/12° [41]
Vehicle/Barrier (Tx/Rx)	Omni	5.3 dBi	360°/20° [42]

In the sedan test (Fig. 4(a)), the vehicle antenna is mounted on the roof-top of the vehicle, 0.3m from the front windshield, at a height of 1.5m (Fig. 4(b)). The radio is secured inside the vehicle. At the receiver end, two barrier antennas are installed 10 m behind the impact point, with heights of 0.82m (generic barrier height) and 1.5m (roof-top height of the vehicles), respectively. The placement and directivity of the vehicle and barrier antennas in these two crash tests are illustrated in Fig. 2, where the barrier antenna(s) are placed off the vehicle trajectory due to safety considerations.

In the pickup test (Fig. 2(c)), the vehicle antenna is mounted on the roof-top of the vehicle similar to the sedan test. The height of the pickup is 1.85 m and the antenna is placed 0.3 m behind the front windshield. The barrier antennas are placed on the barrier 14m before the crash point. Two omni-directional antennas are placed at barrier height (0.78 m) and 1.98 m, respectively, and a directional antenna is placed at 1.85 m height, as shown in Fig. 2(c).

To provide guidance for the specifics of future V2B systems, a combination of directional and omni directional antennas are used on the vehicles and the barriers. Directional antennas significantly enhance communication range, while they need to be well-aligned to ensure their main beam is covering the encroaching vehicles. Barriers are mainly located on the roadside. Hence, it is reasonable to assume that to enhance communications, barrier antennas will have some directivity to focus the emitted electromagnetic waves towards the road. On the vehicle side, directional antennas are used in bogie and sedan tests to ensure connectivity. Moreover, in the pickup test, omni-directional antennas are used in the vehicle, while both omni and directional antennas are used at the barrier. The impacts of directivity of antennas are discussed in Section 4.

The OFDM communication system in the experiment has a baseband sampling rate of 500 ksps, FFT length of $N_{FFT} = 64$, cyclic prefix length of $N_{CP} = 128$, and modulation of BPSK, which mostly reflect DSRC physical layer parameters.[2] The frame structure of OFDM signal is illustrated in Fig. 7. In the frequency dimension, there are 8 guard subcarriers at the upper and lower edges, respectively. In the temporal dimension, each frame has 25 OFDM symbols: a preamble symbol followed by 24 data symbols. In the preamble symbol, a specific sequence is transmitted on odd subcarriers, while all even subcarriers are nulled. In data symbols, subcarriers 32, 33 are nulled for DC. We define subcarrier set, D_p, as the indices of occupied subcarriers in preamble, and D_d as the indices of occupied subcarriers in data symbol, and E_p and E_d as indices of nulled non-guard subcarriers in preamble and data symbols, respectively. Each data frame contains a total of 138 bytes including a

2 DSRC uses a higher bandwidth which is not possible due to equipment limitations.

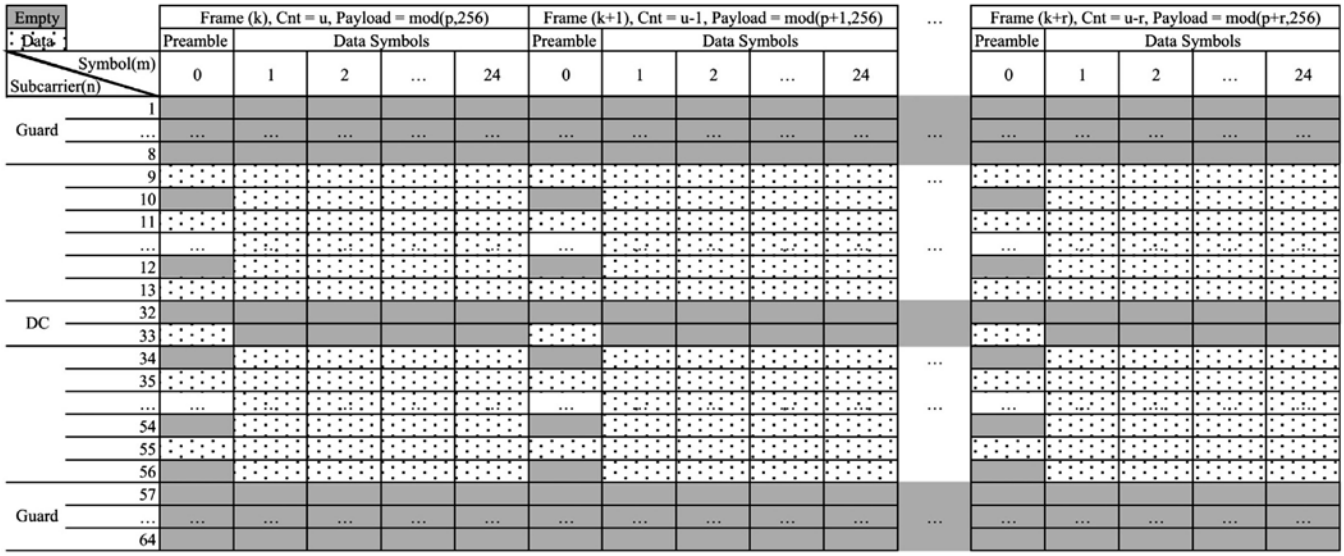

Fig. 7. OFDM frame structure for the experiments

header, payload, and pilots. The header includes a 16-bit counter that is decreased by 1 every frame. The payload is only 1-byte with value of $p = mod(k, 256)$, repeated at 7 locations (7, 9, 11, 18, 32, 39, 67) out of the 138 bytes. The remaining 129 bytes have constant values and are all treated as pilots.

The instantaneous acceleration of the vehicle during experiments is measured by a 9-axis motion tracking sensor, MPU-9150, which is integrated into USRP E312. Acceleration in 3-axes is collected with a sample rate of 9 Hz for all these experiments. In this paper, only the acceleration on the axis of vehicle motion is reported since it is relevant to the crash tests. The velocity and position of the test vehicle are measured by AMY-6M GPS module integrated into USRP E312 at a sample rate of 1Hz. The GPS antenna is installed on top of the bogie and rooftop of the sedan and pickup. Besides on-board sensors, a high-definition camera affixed to the receiver records the vehicle encroachment and crash.

The accelerometer sensory data is time-stamped on-the-fly during the experiments. With the time-stamped video recording, IQ data, and acceleration data, the crash moment is identified. Accordingly, the timing of received IQ data is recovered offline.

3.2. Channel equalization and demodulation

The recorded IQ data at the receiver is after frequency and time synchronization, and in the frequency domain. Offline signal processing includes channel equalization, demodulation, and timing recovery.

First, the preamble of each frame is identified according to following criteria:

$$\frac{\sum_{i\in Dp} |S_i|^2}{\sum_{i\in Dp\cup Ep} |S_i|^2} > \theta \tag{1}$$

where $S_i = I_i + Q_i j$, ($j = \sqrt{-1}$) is the complex representation of sample IQ data on the ith subcarrier, and θ is a threshold, defined as 0.5 in this paper. Once the preamble is identified, we use it as pilots to perform Least Square channel equalization [44] to the first data symbol. The preamble (Fig. 7) is viewed as comb-type pilot, for which linear interpolation is employed in channel estimation. Then, the rest of data symbols are processed iteratively: The entire demodulated 46 subcarriers of data symbol m, treated as block-type pilot, are used to estimate the channel coefficients and equalize data symbol $m + 1$. Based on the known pattern of the data in a frame, erroneous bits in data symbol m are corrected before being used as pilot for channel estimation.

With equalized IQ data, the frame header and payload are then demodulated and decoded. Since the OFDM receiver we used drops a data frame if it fails to synchronize and identify preamble, some data frames are missing in the received IQ data. The decoded decremental frame identifier in the frame header is then used to identify the missing OFDM frames and recover the timing of received IQ data accordingly. For example, if frame k in the received data is followed by frame $k + 3$, then we conclude that frames $k + 1$, $k + 2$ are missing.

The estimated channel coefficient vector of each OFDM symbol is also recorded and used to calculate the channel coherence time.

3.3. Performance metrics

The experimental V2B communication link is evaluated based on IQ data before and/or after equalization. Performance metrics used in the evaluation include: received signal strength (RSS), signal-to-interference- plus-noise ratio (SINR) [45], error vector magnitude (EVM), phase error (PE), and bit error rate (BER).

The RSS of an OFDM symbol is calculated by:

$$RSS = 10 \log_{10} \frac{\sum_{i=1}^{N_{FFT}} |S_i|^2}{T_s} + c \tag{2}$$

where c is calibration constant converting received power from digital domain (*dBFS*) to analog domain (*dBm*), and T_s is the length of an OFDM symbol

in time. For the USRPs used in the experiments, c, is measured as 100.999 in advance. T_s is calculated as:

$$T_s = \frac{N_{FFT}}{f_s} \tag{3}$$

where f_s is the base band sampling rate.

For SINR, the 24 nulled subcarriers in preamble are used to calculate the noise plus interference power, and 24 pilot subcarriers in preamble are used to calculate the signal power. The SINR before and after equalization are calculated based on following equation:

$$SINR = 10 \log_{10} \left(\frac{\sum_{i \in Dp} |S_i|^2}{\sum_{i \in Ep} |S_i|^2} \right) \tag{4}$$

EVM measures the relative magnitude of the error vector between IQ data sample and its expected value (reference) in the constellation [35]. We calculate the RMS of EVM in dB for each OFDM symbol as:

$$EVM_{rms} = 10 \log_{10} \left(\frac{1}{N_D} \sum_{i \in D_d} \frac{|S_i - S_{ref,\,i}|^2}{|S_{ref,i}|^2} \right) \tag{5}$$

where $S_{ref,\,i}$ is reference constellation points on subcarrier i. The values of reference points in BPSK modulation are $S_{rms}(1 + 0j)$ and $S_{rms}(-1 + 0j)$, where S_{rms} is the root mean square of the data samples $\{S_i,\ i \in D\}$, corresponding to the average amplitude of occupied subcarriers in an OFDM symbol of the equalized received IQ data.

The RMS PE of an OFDM symbol of the equalized IQ data is calculated as:

$$PE_{rms} = \sqrt{\frac{1}{N_D} \sum_{i \in D} (\angle S_i - \angle S_{ref,i})^2} \tag{6}$$

where $\angle$ is the angle of a sample of IQ data.

To evaluate the channel coherence time, we also calculate the correlation coefficient between channel estimate vectors of each data symbol and the preamble in each frame.

4. Experiment results

In this section, we first present the communication experiment results of the three crash tests: 1) Bogie Test, 2) Sedan Test, and 3) Pickup test. Metrics discussed in Section 3.3, RSS, SINR, EVM, PE, coherence time, symbol missing rate (SMR), frame bit error rate, and BER are presented. Then, based on these results, an in-depth analysis of the impact of antenna height and directivity, vehicle type and mobility on the channel characteristics is provided in Section 4.4.

To compare the characteristics of communication at different phases of the crash test, five intervals with distinct distance, speed and acceleration are emphasized. The crash time is referred to $t = 0$. These intervals are listed in Table 2, and described as follows:

- *Pre-crash stationary*: During this interval, the vehicle is static at the initial location. The transmitter is far from the receiver. This interval is selected to compare with the other three to study the influence of vehicle velocity and crash on communication quality.
- *Pre-crash moving*: During this interval, the moving vehicle is about to crash to the obstacle. This interval is important for V2B communications because any crash avoidance-related communication may be conducted at this time.
- *Peri-crash*: This interval includes the period of crash, with a drastic change in acceleration and velocity, as well as vibration caused by physical impact.
- *Post-crash*: This interval is right before the vehicle fully stops after the crash. The vehicle is almost stationary, and the transmitter is close to the receiver. It provides a good comparative metric to evaluate the Doppler effects.
- *Post-crash stationary*: This interval is when the vehicle fully stops after the crash. The vehicle is completely stationary. Therefore it is very similar to the pre-crash stationary interval except for a shorter

Table 2. Selected intervals of crash tests (Unit: s).

Interval	*Bogie test*	*Sedan/pickup test*
Pre-crash stationary	[− 19.5, − 18.5]	[− 19.5, − 18.5]
Pre-crash moving	[− 2, − 1]	[− 2, − 1]
Peri-crash	[− 0.5, + 0.5]	[− 0.5, + 0.5]
Post-crash	[+ 2, + 3]	[+ 4, + 5]
Post-crash stationary	N/A	[+ 18.5, + 19.5]

distance. This interval is used for omni-antenna receivers as an alternative of pre-crash stationary, since they do not receive data during pre-crash stationary phase.

4.1. Bogie to post crash test

The vehicle starts moving at $t = -9$ s, is accelerated to 27 mph in a few seconds, then hits the post with a peak acceleration of $-7g$, and completely stops at $t = 3$ s. The RSS aligned with acceleration and speed of the vehicle during the test period are shown in Fig. 8, with highlights of the four intervals listed in Table 2.

The RSS fluctuates between − 76 and − 53 dBm before crash, and converges to − 67.25 dBm peri-crash and post-crash, since the vehicle stays at almost the same location of the impact point. The RSS in postcrash interval decreases 7 dB compared to pre-crash stationary interval despite the shorter distance between barrier and vehicle antenna. It is because throughout the test the highly directional barrier antenna is pointed to the initial location of the vehicle with a directional antenna. As the vehicle approaches, the antenna gain of the link decreases due to the increased mismatch in directivity. On the other hand, when vehicle is at longer distances, e.g. initial location or moving, the radio signal experiences more fading than closer or stationary. The fluctuation of RSS is more intense when vehicle is far away ($t < -9$), than post-crash ($t > 3$), and also faster when vehicle is moving ($-8 < t < 0$) than stationary.

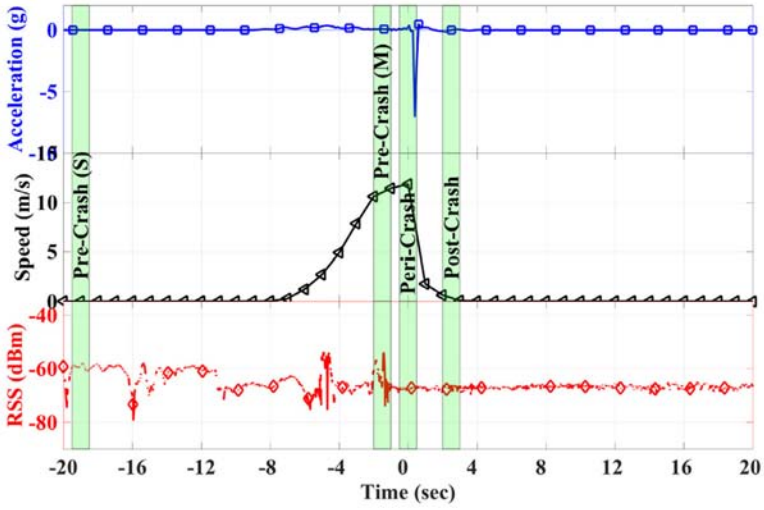

Fig. 8. Acceleration, velocity, and RSS in the bogie test, antenna height 0.9 m.

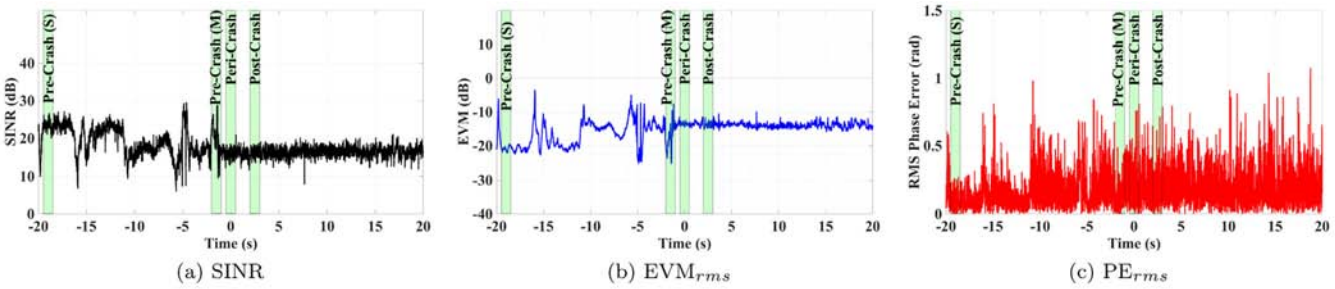

Fig. 9. Overall OFDM signal impairments during the bogie test after channel equalization.

Due to the decreasing RSS, the SINR, EVM, and PE also get worse when the vehicle approaches, as illustrated in Figs. 9. At t= −16, −15, −11, −5, −2 s, the drastic changes of SINR, EVM and PE also correspond to fluctuations of RSS. This results show that the overall signal quality is mainly determined by RSS.

The SINR in the bogie test, as illustrated in Fig. 9(a), is initially high with a typical value of 21 dB with occasional drops. During the traveling period $-9 < t < -1$, the SINR fluctuates more drastically around 17 dB with a dynamic range of 2–30 dB. The fluctuation of RSS and SINR during the traveling period is caused by shadow fading, of which the traveling distance of the two peaks in Fig. 9(a) ($-6 < t < -4$, and $-2.5 < t < -1.5$) is around 5 m, which is significantly smaller than the sedan and pickup tests, where the typical traveling distance of a peak is around 20 m. The smaller shadow fading characteristics in bogie test can be attributed to the lower vehicular antenna height (0.9 m) due to smaller body size and different shape. However, SINR peri and post-crash is around 16 dB with significantly less fluctuations, as vehicle and barrier antennas are both stationary and at shorter distances.

EVM_{rms} in the bogie test exhibits similar pattern as SINR and RSS, as shown in Fig. 9(b). The initial EVM in the pre-crash stationary phase is typically −21 dB, and during the traveling period, it fluctuates between −23 and −4 dB, and converges to around −10 dB peri and post-crash. PE_{rms} fluctuates between 0–1.07 rad, and is typically smaller than 0.5 rad, as shown in Fig. 9(c). The envelope of PE_{rms} varies according to RSS, SINR, and EVM. The average value of PE_{rms} increases as SINR decreases.

The CDFs of SINR, EVM, and PE in the four highlighted intervals are presented in Fig. 10. The SINR, EVM and PE, all perform best in the Pre-Crash Stationary interval, due to high RSS, and they also have the largest dynamics during the pre-Crash Moving interval caused by the small scale

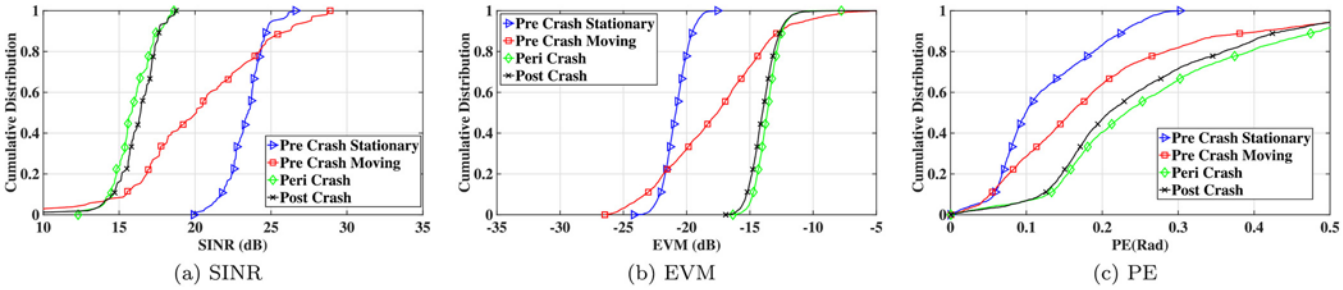

Fig. 10. OFDM signal impairments in CDFs in the bogie test after channel equalization.

fading captured by this interval. Their distributions during peri-Crash and post-Crash are similar compared to the other two intervals. Interestingly, SINR, EVM and PE during the Peri-Crash are always worse than Post-Crash interval (hence the worst among the 4 intervals), despite the locations of vehicle in these two intervals is almost identical. However, this phenomena could not be detected in temporal domain as illustrated in Fig. 9. This small but certain difference between peri-Crash and post-Crash intervals shows that the wireless channel during the crash causes more impairments to OFDM signals. Note that due to missing frames, the CDFs of EVM and PE do not reach to 1.

Channel coherence during the four intervals are presented in Fig. 11(a). Each marker on the curve represents the correlation coefficient between the estimated channel responses of the preamble symbol and a data symbol with specific time offset, averaged over all the frames in an interval. With a correlation threshold of 0.5, the coherence time during pre-crash Stationary, pre-crash Moving, peri-crash, and postcrash intervals are 3.4, 2.3, 1.6, and 1.6 ms, respectively. Lower SINR could contribute to the lower coherence time during Peri-Crash and Post-Crash intervals.

The OFDM receiver drops a frame if it fails to detect or synchronize a preamble. The missing symbols is viewed as a burst error and could be identified after timing recovery. The symbol missing rate (SMR) and BER collected every 5 frames are presented in Fig. 11(b). In the bogie test, only 2.3% of symbols are missing, which indicates low burst error rate. Moreover, errors do not concentrate in a certain time interval. Average BER for bogie test is 3.215%, this BER is generally low and correlated with missing symbols. Since, in the bogie test, only one barrier antenna is used, therefore, we have conducted sedan test with multiple barrier antenna heights. The sedan test results are presented in the next section.

4.2. Sedan to curb crash test

In the sedan test, two co-located barrier antennas are used with heights of 0.82 and 1.5 m, referred as lower and upper barrier antennas, respectively. The sedan test takes in the influence of car body and provides an opportunity to analyze the influence of barrier antenna heights.

RSS aligned with acceleration and speed of the vehicle during sedan test is illustrated in Fig. 11(c), with highlights of the four intervals in Table 2. The vehicle starts moving at $t=-13$ s, accelerates to 15 mph in about 11 s, then hits and crosses over the curb turning slightly to its right, decelerates in a period of 5 s with peak acceleration of −0.9 g, and fully stops after $t = 5$ s.

RSS on lower barrier antenna starts with −53 dBm during pre-crash stationary, and almost keeps unchanged during accelerating. RSS starts to decrease at $t= -5$ s at the end of acceleration period, from −53 dBm to −68 dBm during the encroachment, and fluctuates between −77 and−56 dBm peri-crash. During deceleration, RSS varies between−77 and −35 dBm, and after vehicle fully stops, RSS decreases from −53 to −70 dBm. The decrease of power post-crash is due to the body of sedan blocking the line of sight path between vehicle antenna and the lower barrier antenna. RSS on upper barrier antenna starts with −61 dBm during pre-crash stationary, and converges to−58 dBm post crash after full stop. During the test, it fluctuates between −70 and −35 dBm. The RSS fluctuation is mostly because of shadow fading. Based on the peaks ($-3 < t < -0.5$ on lower barrier antenna, and $-3.5 < t < -1$ on upper antenna), the traveling distance of the vehicle across a peak is about 20 m. The fluctuations of RSS during encroachment, peri-crash and post-crash from two barrier antennas are partially due to the test vehicle passing the main and side lobes of the barrier antennas.

Similar to bogie test, SINR, EVM, and PE on both antennas in the sedan test also vary by the RSS, as illustrated in Figs. 12 and 13. SINR on lower

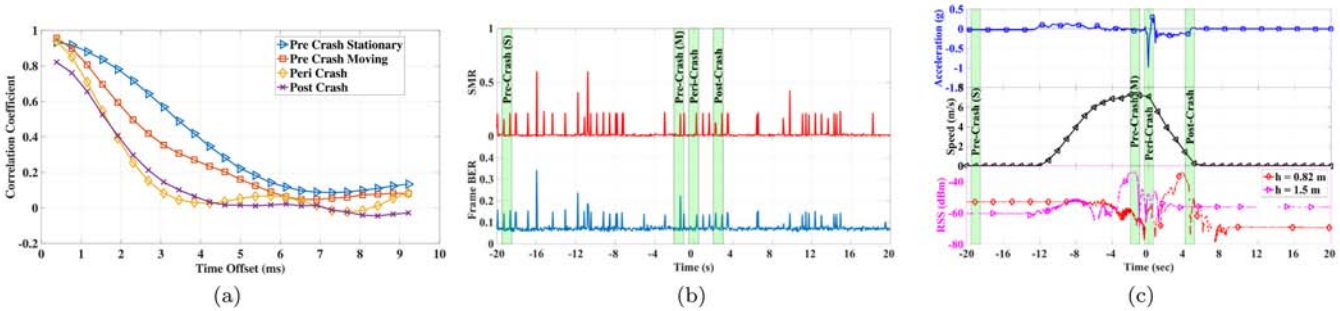

Fig. 11. (a) Channel coherence in the 4 interested intervals of bogie test, (b) BER and symbol missing rate (SMR) of every 5 frames in bogie test, (c) Acceleration, velocity, and RSS on two co-located receivers in sedan test.

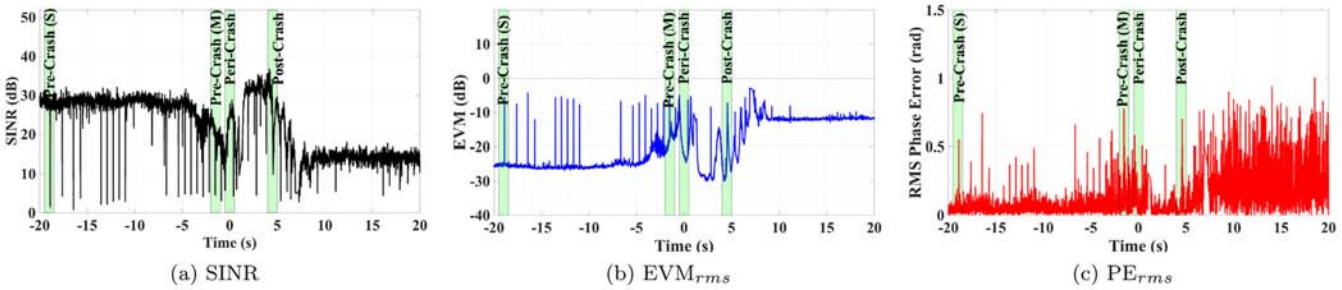

Fig. 12. Overall OFDM signal impairments in sedan test after channel equalization (h = 0.82 m).

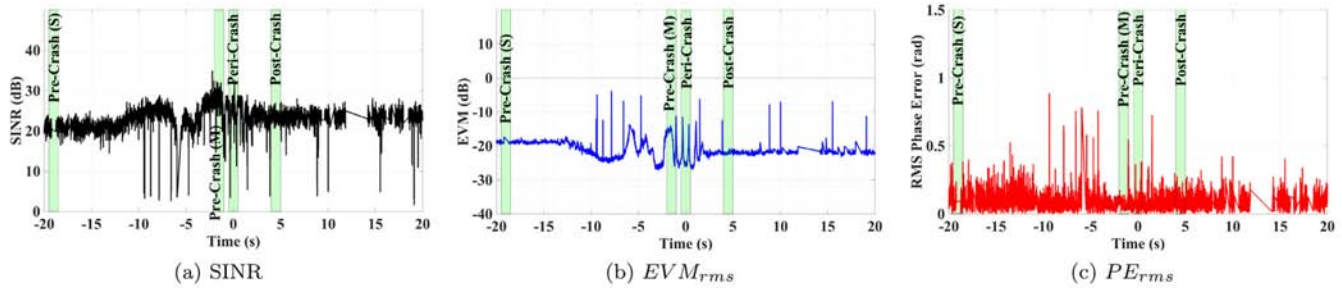

Fig. 13. Overall OFDM signal impairments in sedan test after channel equalization (h = 1.5 m).

barrier antenna is −27 dB in the beginning, and decreases to −15 dBm post crash. SINR of upper barrier antenna is always around 21–23 dB pre- and post-crash when vehicle is stationary. SINR fluctuates between 5 and 34 dB during the test. EVM starts as −26 dB and −19 dB for lower and upper antennas, respectively. RSS in peri-crash fluctuates between−9 and−29 dB for the lower antenna, and between −26 and −18 dBm for upper antenna. RSS converges at −12 and −22 dB for lower and upper antennas, respectively. The variation in PE also echoes with the dynamics of RSS.

CDFs of SINR, EVM, and PE on the lower and upper barrier antennas are shown in Figs. 14 and 15, respectively. For the lower antenna, median SINR in pre-crash stationary and post-crash stationary intervals are 3–10 dB higher than mobile intervals (pre-crash moving and pericrash). Accordingly, median EVM and median PE in stationary intervals is 3–11 dB and 0.04–0.1 rad better than mobile intervals. On the upper antenna, however, it is the opposite: Median SINR in stationary intervals is 1–5 dB lower than mobile intervals. The EVM of mobile intervals has larger variation than stationary intervals. Median PE in pre-crash stationary is 0.3 rad worse than the other 3 intervals due to lower RSS. Variation of PE in peri-crash is larger than 2 pre-crash intervals. Moreover, on both antennas, SINR, EVM and PE in Peri-crash

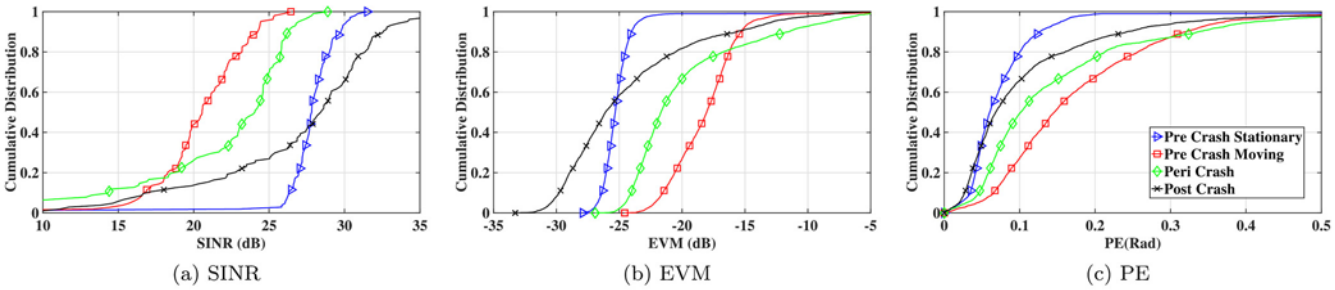

Fig. 14. CDFs of OFDM signal impairments in sedan test with channel equalization (h = 0.82 m).

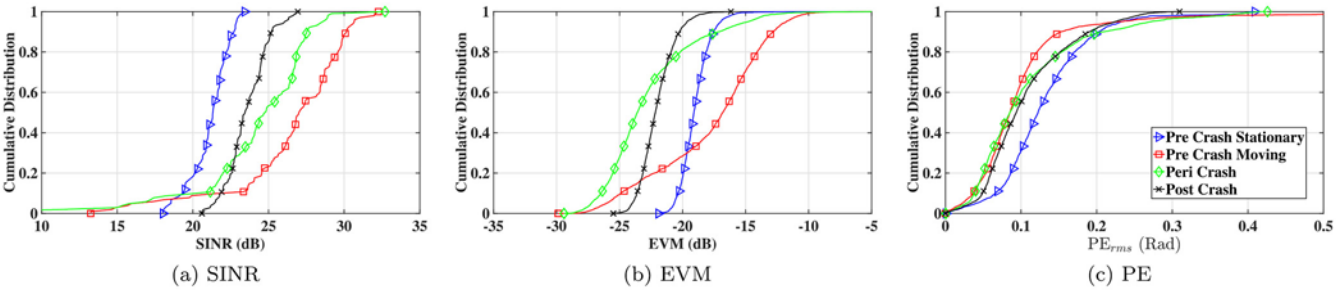

Fig. 15. CDFs of OFDM signal impairments in sedan test with channel equalization (h = 1.5 m).

are not the worst among the 4 intervals in terms of median value, but have the largest variation. This shows that the impairment of signal quality during crash may manifest as larger dynamics.

Channel coherence for the two barrier antennas are presented in Fig. 16. The coherence time of lower antenna (Fig. 16(a)) for pre-crash stationary, pre-crash moving, peri and post crash are 6.2, 2.6, 3.2, and 8.5 ms, respectively. For upper antenna (Fig. 16(b)), the coherence time of the four intervals are 4.6, 4.4, 3.5, and 2.7 ms, respectively. The results show that lower antenna results in high channel coherence time when the vehicle is stationary, but low channel coherence time when the vehicle is moving. It could be explained that signal from moving transmitter to lower antenna may experience more fading than upper antenna due to the effect of ground.

The symbol missing rate (SMR) and BER every 5 frames for the two barrier antennas are shown in Fig. 17(a) and (b). For lower and upper antennas, the overall SMR are 3.5% and 16.7%, respectively, and the overall BERs are 3.090% and 10.53%, respectively. The SMR and BER on upper antenna are 4.7 and 3.4 times higher than those of the lower antenna. This shows that lower barrier antenna consistently outperform upper barrier antenna when other conditions are the same.

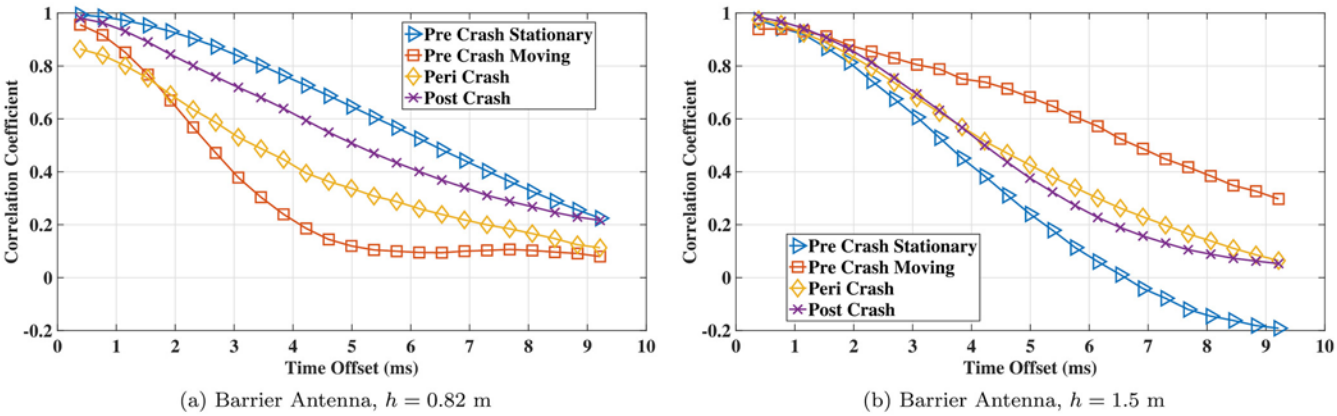

Fig. 16. Channel coherence in 4 intervals for lower and upper antennas in sedan test (a) h = 0.82, (b) h = 0.82 m.

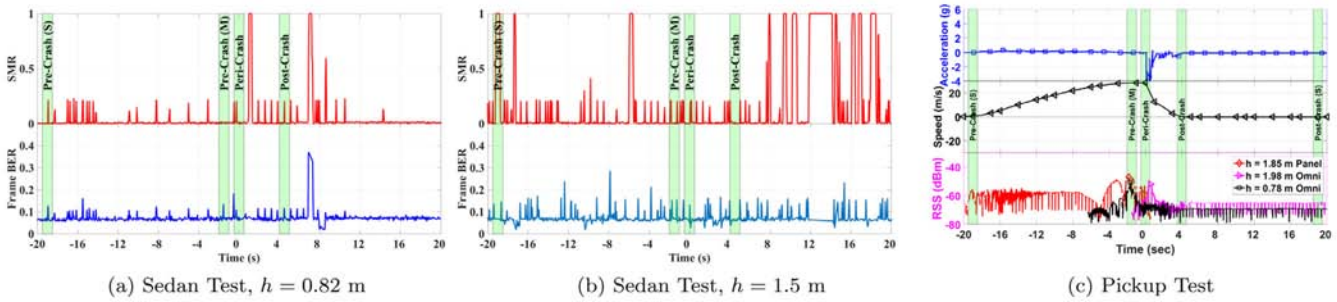

Fig. 17. (a) BER and symbol missing rate (SMR) of every 5 frames in sedan test h = 0.82 m, (b) BER and symbol missing rate (SMR) of every 5 frames in sedan test h = 1.5 m, (c) acceleration, velocity, and RSS on three co-located receivers in pickup test.

4.3. Pickup to steel barrier crash test

In the bogie and sedan tests, both vehicle and barrier antennas are directional. For comparison, we conducted the pickup test, which evaluates the performance of the combinations of omni-directional vehicle antenna, omni-directional and directional barrier antennas. In this test, three barrier receivers are used, two omni-directional antennas with heights of 0.78 m and 1.98 m, respectively, and one directional antenna with height of 1.85 m. The experimental setup is detailed in Section 3.

The pickup starts moving at $t = -18$ s, accelerates to 62 mph at $t = -3$ s, hits the steel barrier at t = 0 s, and then moves along the barrier until it fully stops at t = 5 s. The peak acceleration during the crash is − 5 g. The RSS at three barrier antennas aligned with acceleration and speed of the vehicle during pickup test are shown in Fig. 17(c), with highlights of the four intervals in Table 2. Connectivity of the directional barrier antenna is established

before vehicle starts moving, at a distance of 338 m. Due to lower gain, connectivity of omni-directional antennas is established at shorter distances, specifically, at $t = -6.3$ s and $t = -1.5$ s for lower ($h = 0.78$ m) and upper (1.98 m) antennas before the crash, or about 100 m and 30 m away from the crash point, respectively. However, after the crash, the connectivity of directional barrier antenna is lost as the vehicle is outside the main lobe. This suggests site-specific antenna alignment is necessary for practical V2B deployments.

The RSS at directional barrier antenna during pre-crash stationary is 5.7 − 7.9 dB higher than that at the lower and upper omni-directional barrier antennas. The lower omni antenna RSS varies between − 71 dBm–− 52 dBm between pre-crash static and pre-crash moving phases. However, during post crash, it increases up-to − 42 dBm. The RSS of directional antenna fluctuates between − 60 dBm to − 51 dBm during pre-crash static and pre-crash moving phases. On the other hand, it rises up-to − 41 dBm during peri-crash. When the pickup fully stops, $t \geq 6$ s, RSS at the upper omni-directional barrier antenna is 2 dB higher than the lower omni barrier antenna. It is because the line-of-sight between vehicle antenna and lower omni barrier antenna is partially blocked by the rooftop of the vehicle after crash.

From Fig. 17(c), degradation of RSS can be observed throughout the test. Furthermore, during mobile phases, the RSS also follows a smooth transition between valley and peaks. The degradation in RSS is linked to small scale fading, while the smooth transition is linked to shadow fading, as vehicle travels while barrier antenna is stationary. The highest peaks in RSS for the lower and upper omni barrier antennas occur in pre-crash moving and peri-crash intervals, while the highest peak for directional barrier antenna occurs in the pre-crash moving interval. Based on the peaks ($-3.8 < t < -3.0$ for lower omni barrier antenna, and $-2 < t < -1$ for directional barrier antenna), the traveling distance of the vehicle across a peak is about 21–26 m.

The SINR, EVM, and PE at the three barrier antennas during the test are shown in Fig. 18. For lower omni barrier antenna, SINR varies between 18 dB to 24.5 dB in pre-crash moving, and the peak of SINR (26 dB) is in pre-crash

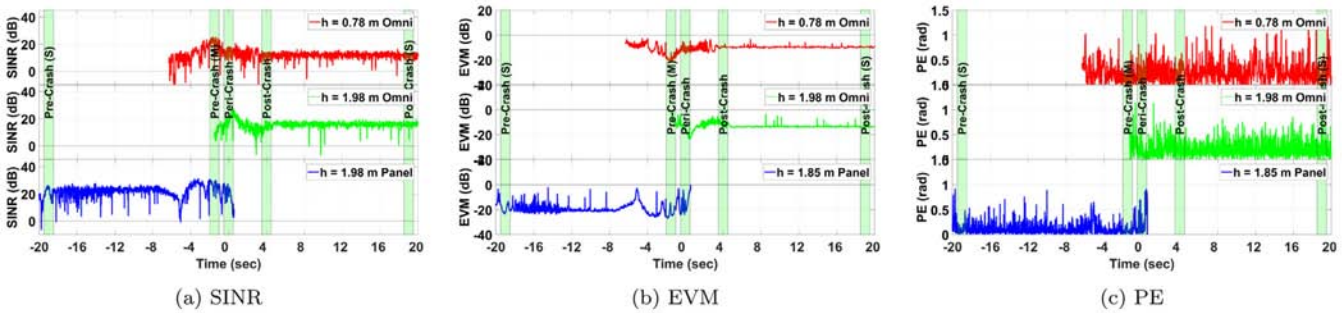

Fig. 18. Over OFDM signal impairments in pickup test for 3 barrier antennas after channel equalization.

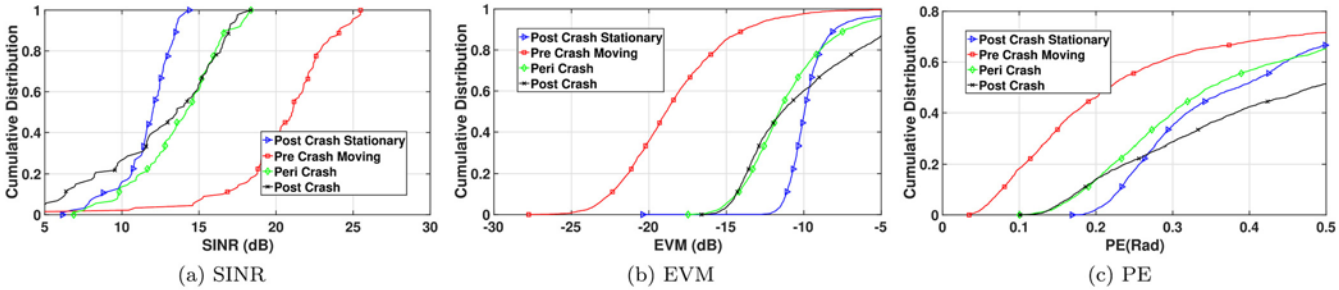

Fig. 19. CDFs of OFDM signal impairments in pickup test with channel equalization (h = 0.78 m).

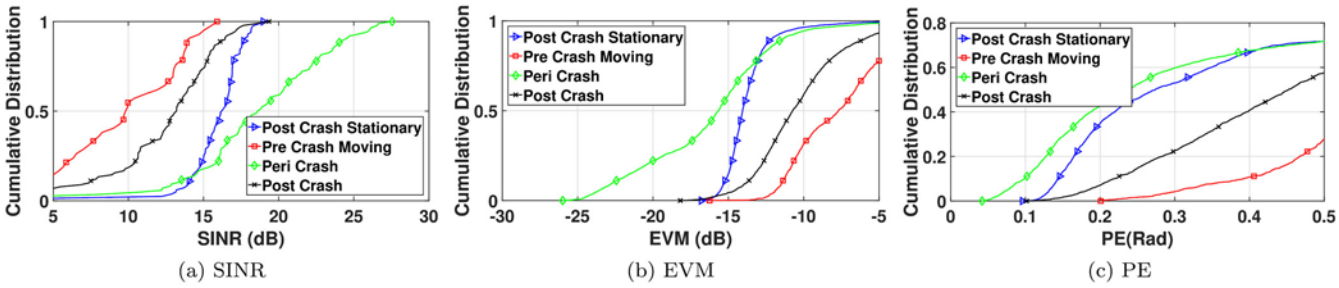

Fig. 20. CDFs of OFDM signal impairments in pickup test with channel equalization (h = 1.98 m).

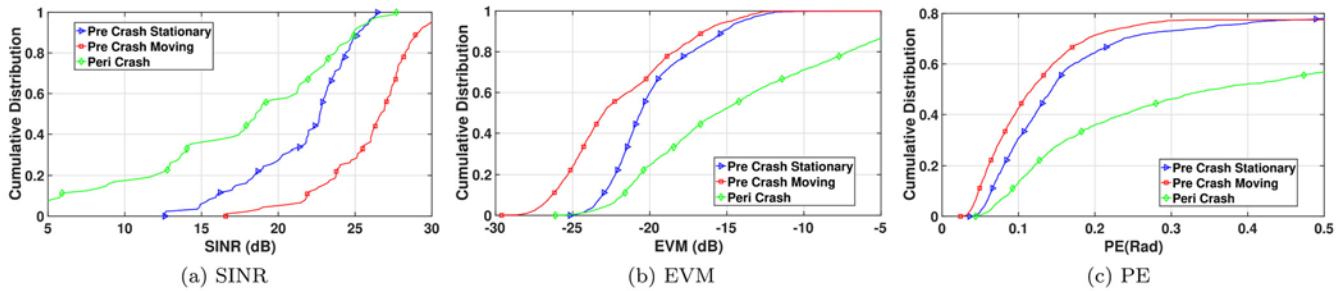

Fig. 21. CDFs of OFDM signal impairments in pickup test with channel equalization (h = 1.85 m).

moving interval. For upper omni barrier antenna, peak SINR (27.5 dB) occurs in peri-crash interval. The peak SINR on directional barrier antenna also occurs in the pre-crash moving interval. Similar to bogie and sedan tests, SINR, EVM, and PE in pickup test also vary by RSS, which is influenced by shadow and small scale fading.

The CDFs of SINR, EVM, and PE at the three barrier antennas during the 4 intervals are illustrated in Figs. 19–21, respectively. Because of shadow fading, CDFs of the metrics for omni barrier antennas are quite different across the 4 intervals. For the lower omni barrier antenna (Fig. 19), the median SINR (EVM) in pre-crash moving is 6–9 dB higher (7–9 dB lower) than the other 3 intervals, and median PE_{rms} in pre-crash moving is 0.1–0.2 rad

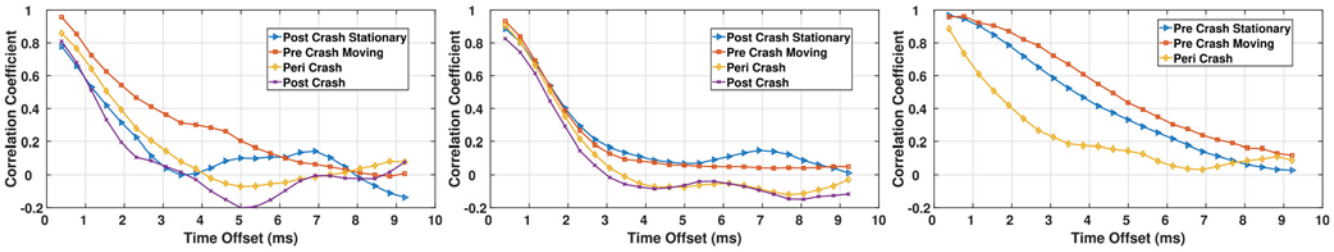

(a) Omni-Directional, h=0.78m (b) Omni-Directional, h=1.98m (c) Directional, h=1.85m

Fig. 22. Channel coherence of 4 intervals for lower and upper barrier antennas in pickup test.

lower than the rest. For the higher omni barrier antenna (Fig. 20), the SINR (EVM) in peri-crash interval is 2–7 dB higher (2–8 dB lower) than the other 3 intervals, and median PE_{rms} in pre-crash moving is 0.01–0.45 rad lower than the rest. Moreover, the variance of the metrics in peri-crash interval close to other intervals. Therefore, the impairment effects on omni barrier antennas in pericrash is insignificant. For directional barrier antenna, the variance of SINR, EVM, and PE in peri-crash intervals are significantly higher than the other two intervals despite the dynamic range of RSS peri-crash is between the other two intervals. This impairment pattern is similar to the bogie and sedan tests. Note that the vehicle enters in the side lobes of the directional barrier antenna in peri-crash interval, and then the connectivity is lost as the vehicle moves in the area of the lowest gain.

Channel coherence of the three barrier antennas is illustrated in Fig. 22. Coherence time for lower (upper) omni barrier antenna is 2.1 (1.8) ms during pre-crash moving, and 1.5 (1.7) ms during post crash. For directional barrier antenna, the coherence times are 4.7, 3.5, 1.6 ms during pre-crash stationary, pre-crash moving, peri-crash intervals, respectively. Note that the coherence time for directional barrier antennas is 1.6–2.7 times that for the omni barrier antenna when vehicle is in the main lobes (pre-crash stationary and moving). However, coherence time for directional barrier antenna is similar (±7%) to the omni barrier antenna in peri-crash interval when vehicle is in the side lobes. Although the crash velocity in the pickup test is 2.29 times higher than in the bogie test, the coherence time in peri-crash interval in pickup test is similar (±7%) to the bogie test.

In Fig. 23 the symbol missing rate (SMR) and BER per frame for the three barrier antennas are illustrated. During pre-crash moving interval, average SMR for lower omni, upper omni, and directional antennas are 16.36%, 33.85%, and 12.73%, respectively. Therefore, when vehicle to three barrier antennas are the same, SMR of directional barrier antenna is 23% and 63% lower than lower and upper omni-directional barrier antennas. However, in peri-crash interval, average SMR of these barrier antennas are 16.19%,

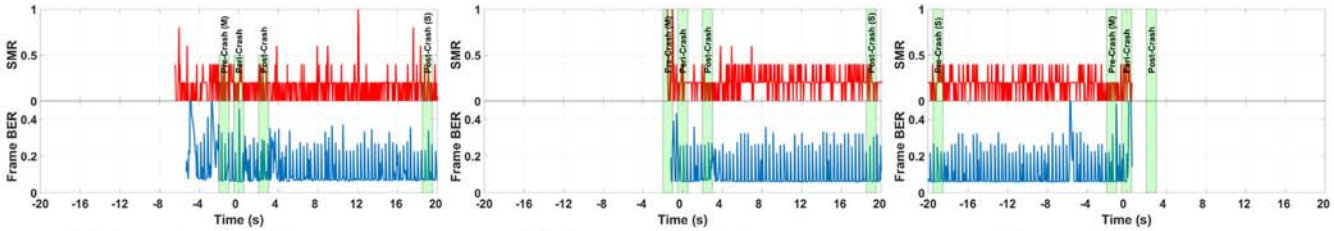

(a) Omni-Directional, $h = 0.78$ m (b) Omni-Directional, $h = 1.98$ m (c) Directional, $h = 1.85$ m

Fig. 23. BER and symbol missing rate (SMR) of every 5 frames for barrier antennas in pickup test.

18.18%, and 17.27%, respectively. During the crash, the difference of signal quality at the three antennas is insignificant. In stationary intervals (post-crash for omni barrier antennas, and pre-crash stationary for directional barrier antenna), the average SMR are: 11.82%, 20.91%, and 20%, respectively. In pre-crash stationary intervals, communication distance of directional barrier antenna is 9.6 times longer than that of the omni barrier antenna. In post-crash stationary interval, the SMR for directional barrier antenna is 69% higher than the lower omni barrier antenna, and 5% lower than upper omni barrier antenna. These results show that directional barrier antenna improves signal quality when vehicle is in its main lobes compared to omni barrier antenna, however, directional barrier antenna faces more impairments than omni antennas at short distances.

It can be observed that panel antennas are useful to establish communication at longer distances and careful alignment is necessary for short distance communications. Omni antennas are suitable in scenarios where longer distances may not be desired (lower speeds) or directional antennas can not maintain connectivity because of a curve or in close vicinity of a physical barrier. For omni barrier antennas, smaller antenna height leads to better signal quality than larger antenna height in V2B communications. In the next section, a summary of the findings of all three crash test results is presented.

4.4. Summary and discussion of the three crash test results

We summarize the RSS, SINR, EVM, and PE results in the 5 predefined intervals (pre-crash stationary, pre-crash moving, peri-crash, post-crash, and post-crash stationary) in Table 3 for the first two tests with directional vehicle antenna, and in Table 4 for the third test with omni-directional vehicle antenna. The impacts of vehicle and barrier antenna directivity, antenna height, propagation environment, and mobility on the characteristics of V2B channel are discussed as follows.

Table 3. The average signal quality in four intervals of the two directional vehicle antenna-barrier antenna crash tests with equalization.

Phase	*RSS (dBm)*			*SINR (dB)*			*EVM (dB)*			*PE (rad)*		
	Bogie	*Sedan*		*Bogie*	*Sedan*		*Bogie*	*Sedan*		*Bogie*	*Sedan*	
	0.9 m	*0.82 m*	*1.5 m*	*0.9 m*	*0.82 m*	*1.5 m*	*0.9 m*	*0.82 m*	*1.5 m*	*0.9 m*	*0.82 m*	*1.5 m*
Pre-crash stationary	−59.335	−52.889	−60.284	23.37	27.72	21.17	−20.83	−25.09	−18.98	0.088	0.052	0.100
Pre-crash moving	−62.890	−62.419	−56.080	20.16	20.49	26.55	−17.68	−18.13	−17.79	0.127	0.135	0.065
Peri-crash	−67.249	−60.240	−52.201	15.92	22.13	24.21	−13.63	−19.95	−22.74	0.196	0.111	0.088
Post-crash	−66.954	−45.678	−61.695	16.25	26.88	23.58	−13.95	−28.68	−22.33	0.172	0.038	0.083

Table 4. The average signal quality in five intervals of the omni-directional vehicle antenna-directional/omni barrier antenna crash tests with equalization.

Phase	*RSS (dBm)*			*SINR (dB)*			*EVM (dB)*			*PE (rad)*		
	Directional	*Omni-directional*		*Directional*	*Omni-directional*		*Directional*	*Omni-directional*		*Directional*	*Omni-directional*	
	1.85 m	*0.78 m*	*1.98 m*	*1.85 m*	*0.78 m*	*1.98 m*	*1.85 m*	*0.78 m*	*1.98 m*	*1.85 m*	*0.78 m*	*1.98 m*
Pre-crash stationary	−59.924	–	–	21.325	–	–	−19.439	–	–	0.097	–	-
Pre-crash moving	−51.670	−57.393	−71.612	26.578	20.410	10.015	−22.787	−18.322	−7.782	0.069	0.154	0.432
Peri-crash	−63.245	−68.255	−61.998	19.016	13.748	18.720	−15.662	−11.105	−16.351	0.244	0.226	0.156
Post-crash	–	−69.427	−67.878	–	11.921	13.525	–	−9.763	−11.505	–	0.280	0.232
Post-crash stationary	–	−65.591	−67.878	–	11.627	15.928	–	−9.613	−13.688	–	0.233	0.196

Environmental complexity is one of the major determinants of channel characteristics. The BER and symbol missing rate (SMR) of the bogie test (Fig. 11(b)) exhibit less fluctuations compared to the sedan test (Fig. 17(a) and (b)) despite the fact that similar configurations of transmitters and receivers are employed in these two tests. This can be explained by more intensive small scale fading in a richer multi-path environment of the second test. Interestingly, although the pickup test is conducted in a similar environment as the bogie test, its BER and SMR show significantly more fluctuations than the first two experiments. Such degradation can be attributed to more severe small scale fading caused by more richer multi-path components when omni-directional vehicle antenna is employed.

The influence of antenna directivity on V2B channel is further illustrated by channel coherence time. In the pre-crash intervals of the pickup test, the coherence time of higher omni-directional barrier antenna (h = 1.98 m) is only about half that of the directional barrier antenna (h = 1.85 m) despite the fact that their heights are only 0.13 m apart and the signals are from the same vehicle antenna. It shows that less small scale fading is caused by fewer multi-path components when vehicle antenna is in the main lobe of the directional barrier antenna. In fact, the two omni-directional barrier antennas

have similar coherence time despite the difference in their heights. However, in the peri-crash interval, only when the vehicle antenna is in the side lobes of the directional barrier antenna, the coherence time becomes similar to that of the omni-directional barrier antennas.

Higher mobility of vehicle also reduces the channel coherence time because of lower similarity of propagation environments over unit time. The velocity of vehicle in the bogie test is 80% higher than the sedan test, accordingly, coherence time in bogie test is 58%–64% of the sedan test. Moreover, during crash, the mobility and orientation of vehicle would experience drastic and complex variations on its pitch, roll, and yaw axes compared to regular encroachment. Such irregular movements would cause mismatch in directivity between vehicle and barrier antennas, even for omni-directional vehicle antennas with a narrow vertical beam-width. Therefore, significant degradation of signal quality and channel coherence time in peri-crash interval are observed in the first two tests where both vehicle and barrier antennas are directional. This also explains the severe signal degradation in bogie test with more intensive impact than the sedan test. The directivity mismatch during crash could be reduced significantly by using omni-directional antennas on both vehicle and barriers. As a result, we did not observe significant degradation in signal quality during peri-crash for the omni-directional receivers of the pickup test.

Antenna height also plays an important role in V2B communications. With similar heights, the BERs of 0.9m barrier antenna in bogie test (3.215%) is close to that of 0.82 m barrier antenna in sedan test (3.090%). However, BER of 1.5 m barrier antenna in sedan test is over 3 times higher (10.53%) than that of the lower one (0.82 m). Similar patterns are observed in the pickup test, where BERs of upper directional and lower omni-directional barrier antennas are 3.92% and 7.19%, respectively. However, for upper omni barrier antenna, BER is 4 times higher than that of the lower omni antenna. Moreover, in the pickup test, connectivity of the lower omni-directional antenna is established at much longer distances (∼100 m) than the upper omni antenna (∼30 m). These results show that barrier antenna height plays an important role in V2B communications. For low antenna heights, higher electromagnetic wave energy is reflected from the road surface since the angle of incidence is larger. This finding could be exploited in the design of V2B systems.

The BERs of the three tests are further summarized in Fig. 24, where the entire data reception is divided into four periods. Static: from the beginning to just before the start of car, Moving: from the start of the vehicle to just $t = -2$ s, Crash: from $t = -2$ s to $t = 5$ s, and Stop: from $t = 5$ s to $t = 12$ s. For fair comparison of the three antennas, we exclude the missing data at 12 − 14 s due to human activities after vehicle fully stops. The BER for crash interval of the upper barrier antenna for sedan test is about 18% higher than

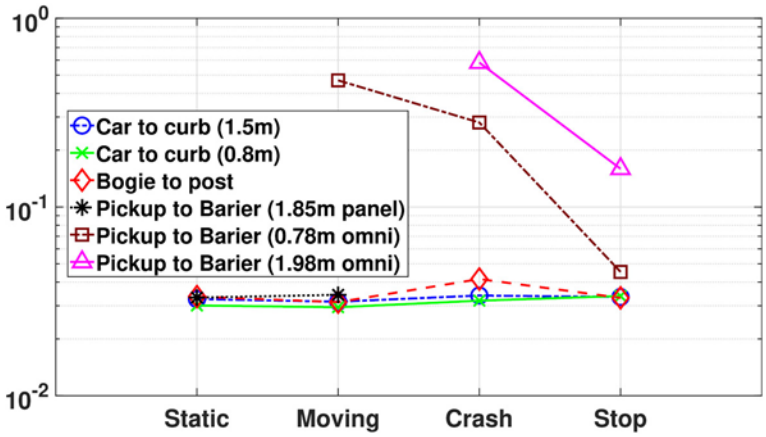

Fig. 24. BER of 4 phases in bogie and sedan crash tests.

the other two lower barrier antennas for bogie and sedan tests, while the BER in other 3 periods of the three barrier antennas for these two tests are very close. On the other hand, in the pickup test, omni barrier antennas have 15 and 18 times higher BER compared to that of directional antenna during moving phase. This high BER proves that omni barrier antennas face higher multi-path effects than directional antennas.

The three tests show that directional antennas on either vehicle or barrier is able to significantly improve the communication distance and channel coherence time of V2B systems when vehicles travel normally, while causing significant adverse effects during an accident, or when vehicle moves into the side lobes at shorter distances. On the other hand, omni-directional vehicular and/or barrier antennas would introduce significantly more multi-path effects and small scale fading, and reduce communication distances. However, it is more robust during an accident. Such additional effects of antenna directivity should be considered for different V2B applications. For example, highly directional barrier antennas could be used for broadcasting road conditions on straight highways, while omni-directional barrier antennas can be used for issuing safety critical signals to inbound and outbound traffics at short distances, and/or on sharp curves and intersections. Furthermore, our test results show that deploying barrier antennas at near barrier height could improve signal quality compared to larger antenna heights.

4.5. Impacts of channel equalization

Compared to [39], in this paper, we present the experiment results following LS channel equalization as discussed in Section 3.2. The LS channel

Table 5. The average signal quality in four intervals of the two directional vehicle antenna-barrier antenna crash tests without equalization.

Phase	*RSS (dBm)*			*SINR (dB)*			*EVM (dB)*			*PE (rad)*		
	Bogie	*Sedan*		*Bogie*	*Sedan*		*Bogie*	*Sedan*		*Bogie*	*Sedan*	
	0.9 m	*0.82 m*	*1.5 m*	*0.9 m*	*0.82 m*	*1.5 m*	*0.9 m*	*0.82 m*	*1.5 m*	*0.9 m*	*0.82 m*	*1.5 m*
Pre-crash stationary	−59.335	−52.889	−60.284	23.32	27.80	21.04	−5.23	−2.45	−3.78	0.685	0.693	0.698
Pre-crash moving	−62.890	−62.419	−56.080	20.22	20.53	26.47	−3.27	−3.24	−2.99	0.716	0.682	0.704
Peri-crash	−67.249	−60.240	−52.201	16.00	22.23	24.26	−2.65	−4.99	−3.03	0.702	0.685	0.668
Post-crash	−66.954	−45.678	−61.695	16.44	31.46	23.93	−6.19	−2.43	−3.05	0.657	0.687	0.717

equalization helps us to demodulate and decode the raw IQ data, and then recover its frame structure. Based on the timing information of the frame header, numerous missing chunks in the raw data are discovered and their lengths are identified. This helps us recover the correct timeline of the received signal, and identify the correct intervals of the signal for each stage of the test. For example, the crash moments in the Bogie and sedan tests after timing recovery is corrected 0.2 and 0.1 s backward, respectively. Meanwhile, temporal resolution is improved from seconds in [39] to milliseconds in this paper.

The average RSS, SINR, EVM, and PE of the four intervals after (Table 3) and before (Table 5) equalization are compared, with correct timing on both equalized and unequalized signals. We can find that the EVM is improved −16.37 dB on average, and PE on average is improved to only 12–21% of the unequalized results. Especially, without equalization, PE exhibit periodical fluctuation which could lead to a significant difference on the average PE of an 1 s interval with a shift of only a few hundreds of milliseconds [39]. However, equalization does not influence RSS and has little impact (0.04 dB–0.19 dB) on the SINR.

Higher time resolution also reveals the impact of the environment. The bogie test is conducted in an open, clean environment, while sedan test is conducted in a more complex environment with more buildings, static objects, and moving personals and vehicles. As a result, deeper fading in a more complex environment causes more spurious degradation of performance metrics and packet losses. For example, symbol missing rate increases from 2.3% in the bogie test to 3.5% (16.7%) for the 0.82 m (1.5 m) antenna in the sedan test. Moreover, it can be observed from Figs. 12, 13, and 17, that the spurious effects are not strongly correlated with lower SINR. For V2B communication, it implies that road traffic could significantly influence the communication quality. These environmental dynamics should be considered in the design of communication protocol.

5. Conclusions

Vehicle to barrier (V2B) communication system is a new addition to the family of V2X communication approaches, aiming to enhance transportation safety. To guide the development of V2B communication solutions, in this paper, real-world crash test results are presented, which reveal the effects of the vehicle crash on OFDM signal transmission on the 5.8 GHz band.

Besides environmental complexity and vehicle mobility, antenna height and directivity are also found to have a significant influence on the characteristics of V2B channels. Experiment results consistently show that barrier antennas deployed at barrier heights (0.82–0.90 m) have better signal quality, longer communication distances, and longer channel coherence times than larger antenna heights (1.5–1.98 m), due to larger angle of incidence at the ground-air interface. Moreover, for vehicles traveling normally, directional barrier and vehicle antennas not only increase the communication distances but also reduce multipath effects and hence, small scale fading. As a result channel coherence time can be significantly increased when directional antennas are employed. These improvements, however, may be traded off during runoff- road crashes due to directivity mismatches caused by drastic changes of vehicle orientation and accelerations. As a result, deployment of directional barrier antennas needs to be accomplished with care. In contrast, omni-directional antennas suffer from shorter distances and multi-path fading but are not significantly affected at short distances. Accordingly, these findings can be exploited in the development of new solutions to prevent run-off-road accidents and/or mitigate the fatalities and injuries.

Acknowledgments — This work is partly supported by NSF CNS-0953900, CNS-1247941, DBI-1331895, and CNS-1423379 awards. The crash tests described in this paper are conducted under the National Strategic Research Institute Contract FA4600-12-D-9000 - Task Order 0055 (TOPR 0002) with funding provided by the US Department of Defense Surface Deployment and Distribution Command Transportation Engineering Agency (SDDCTEA). The data discussed in this paper are ancillary to the data collected for SDDCTEA, and SDDCTEA's support in the data collection effort is greatly appreciated. The authors also would like to acknowledge the support of the project leadership team from the Nebraska Transportation Centers Midwest Roadside Safety Facility (MwRSF), for their help in the data collection effort. Special thanks to Jim Holloway for help in collecting the data at the MwRSF proving grounds.

References

[1] U.D. of Transportation, A compilation of motor vehicle crash data from the fatality analysis reporting system and the general estimates system, Traffic Safety Facts 2013 (2013).

[2] Vehicle-to-vehicle communications: Readiness of v2v technology for application, 2014, https://www.its.dot.gov/cv_basics/pdf/Readiness-of-V2V-Technology-for-Application-812014.pdf Accessed: 2017-10-20.

[3] U.S. Department of Transportation, http://safety.fhwa.dot.gov/roadway_dept/ Accessed: 2016-06-18.

[4] Roadway and environment, http://www.iihs.org/iihs/topics/t/roadway-and-environment/fatalityfacts/fixed-object-crashes/2015 Accessed: 2017-10-20.

[5] NHTSA statistics 2016, https://crashstats.nhtsa.dot.gov/Api/Public/ViewPublication/812451 Accessed: 2018-05-07.

[6] 2015 traffic fatalities, https://www.whitehouse.gov/blog/2016/08/29/2015-traffic-fatalities-data-has-just-been-released-call-action-download-and-analyze

[7] S. Temel, M.C. Vuran, R.K. Faller, A primer on vehicle-to-barrier communications: effects of roadside barriers, encroachment, and vehicle braking, Proc. 2016 IEEE 84th Vehicular Technology Conference (VTC2016-Fall), (2016).

[8] A.F. Molisch, F. Tufvesson, J. Karedal, C.F. Mecklenbrauker, A survey on vehicle-to-vehicle propagation channels, IEEE Wireless Commun. 16 (6) (2009) 12–22.

[9] T. Sukuvaara, P. Nurmi, Wireless traffic service platform for combined vehicle-to-vehicle and vehicle-to-infrastructure communications, IEEE Wirel. Commun. 16 (6) (2009) 54–61.

[10] N. Liu, M. Liu, J. Cao, G. Chen, W. Lou, When transportation meets communication: V2P over vanets, Distributed Computing Systems (ICDCS), 2010 IEEE 30th International Conference on, (2010), pp. 567–576.

[11] R. Hussain, J. Son, H. Eun, S. Kim, H. Oh, Rethinking vehicular communications: merging vanet with cloud computing, IEEE 4th Intl. Conf. on Cloud Computing Technology and Science (CloudCom), (2012), pp. 606–609.

[12] U.S. Department of Transportation, ITS 2015–2019 Strategic plan, Intelligent Transportation Systems (ITS), Joint Program Office (JPO), 2015.

[13] S. Joerer, M. Segata, B. Bloessl, R.L. Cigno, C. Sommer, F. Dressler, A vehicular networking perspective on estimating vehicle collision probability at intersections, IEEE Trans. Veh. Technol. 63 (4) (2014) 1802–1812.

[14] S. Khülmorgen, A. González, A. Festag, G. Fettweis, Improving communication-based intersection safety by cooperative relaying with joint decoding, 2017 IEEE Intelligent Vehicles Symposium (IV), (2017), pp. 679–684.

[15] Q. Wu, L.C.K. Hui, C.Y. Yeung, T.W. Chim, Early car collision prediction in vanet, 2015 International Conference on Connected Vehicles and Expo (ICCVE), (2015), pp. 94–99.

[16] R. Faller, K. Polivka, B. Kuipers, R. Bielenberg, J. Reid, J. Rohde, D. Sicking, Midwest guard-rail system for standard and special applications, Transp. Res. Rec. 1890 (3) (2004) 19–33.

[17] Tesla car that crashed and killed driver was running on autopilot, firm says, https://www.theguardian.com/technology/2018/mar/31/tesla-car-crash-autopilot-mountain-view Accessed: 2018-05-01.

[18] K. Abboud, H.A. Omar, W. Zhuang, Interworking of DSRC and cellular network technologies for V2X communications: a survey, IEEE Trans. Veh. Technol. 65 (12) (2016) 9457–9470.

[19] C.F. Mecklenbrauker, A.F. Molisch, J. Karedal, F. Tufvesson, A. Paier, L. Bernado, T. Zemen, O. Klemp, N. Czink, Vehicular channel characterization and its implications for wireless system design and performance, Proc. IEEE 99 (7) (2011) 1189–1212, http://dx.doi.org/10.1109/JPROC.2010.2101990

[20] W. Viriyasitavat, M. Boban, H.M. Tsai, A. Vasilakos, Vehicular communications: survey and challenges of channel and propagation models, IEEE Veh. Technol. Mag. 10 (2) (2015) 55–66.

[21] T. Abbas, L. Bernado, A. Thiel, C.F. Mecklenbrauker, F. Tufvesson, Measurements based channel characterization for vehicle-to-vehicle communications at merging lanes on highway, IEEE 5th Intl. Symp. on Wireless Vehicular Commun. (WiVeC), (2013), pp. 1–5.

[22] V. Shivaldova, M. Sepulcre, A. Winkelbauer, J. Gozalvez, C.F. Mecklenbruker, A model for vehicle-to-infrastructure communications in urban environments, IEEE Intl. Conf. on Communication Workshop (ICCW), (2015), pp. 2387–2392.

[23] R. Atallah, M. Khabbaz, C. Assi, Multihop V2I communications: a feasibility study, modeling, and performance analysis, IEEE Trans. Veh. Technol. 66 (3) (2017) 2801–2810, http://dx.doi.org/10.1109/TVT.2016.2586758

[24] K.C. Dey, A. Rayamajhi, M. Chowdhury, P. Bhavsar, J. Martin, Vehicle-to-vehicle (V2V) and vehicle-to-infrastructure (V2I) communication in a heterogeneous wireless network–performance evaluation, Transp. Res. Part C 68 (2016) 168–184.

[25] IEEE standard for information technology– local and metropolitan area networks–specific requirements–part 11: Wireless LAN medium access control (mac) and physical layer (phy) specifications amendment 6: Wireless access in vehicular environments, in: IEEE Std 802.11p-2010 (Amendment to IEEE Std 802.11–2007 as amended by IEEE Std 802.11k-2008, IEEE Std 802.11r-2008, IEEE Std 802.11y-2008, IEEE Std 802.11n-2009, and IEEE Std 802.11w-2009), 2010, pp. 1–51, doi:10.1109/IEEESTD.2010.5514475.

[26] M. Segata, F. Dressler, R.L. Cigno, Let's talk in groups: A distributed bursting scheme for cluster-based vehicular applications, Veh. Commun. 8 (Suppl C) (2017) 2–12. Internet of Vehicles

[27] M.A. Togou, L. Khoukhi, A. Hafid, IEEE 802.11p EDCA performance analysis for vehicle-to-vehicle infotainment applications, IEEE Intl. Conf. on Communications (ICC), (2017), pp. 1–6.

[28] X. Wu, S. Subramanian, R. Guha, R.G. White, J. Li, K.W. Lu, A. Bucceri, T. Zhang, Vehicular communications using DSRC: Challenges, enhancements, and evolution, IEEE J. Sel. Areas Commun. 31 (9) (2013) 399–408.

[29] K. Lee, J. Kim, Y. Park, H. Wang, D. Hong, Latency of cellular-based V2X: Perspectives on tti-proportional latency and tti-independent latency, IEEE Access 5 (2017) 15800–15809.

[30] Status of the Dedicated Short-Range Communications Technology and Applications Report to Congress, 2015, http://www.its.dot.gov/index.htm

[31] I. Sen, D.W. Matolak, Vehicle-vehicle channel models for the 5-ghz band, IEEE Trans. Intell. Transp. Syst. 9 (2) (2008) 235–245.

[32] J.C. Lin, C.S. Lin, C.N. Liang, B.C. Chen, Wireless communication performance based on IEEE 802.11p R2V field trials, IEEE Commun. Mag. 50 (5) (2012) 184–191.

[33] L. Cheng, B.E. Henty, D.D. Stancil, F. Bai, P. Mudalige, Properties and applications of the suburban vehicle-to-vehicle propagation channel at 5.9 ghz, Intl. Conf. on Electromagnetics in Advanced Applications, ICEAA. (2007), pp. 121–124.

[34] Y. Zhao, S.G. Haggman, Intercarrier interference self-cancellation scheme for OFDM mobile communication systems, IEEE Trans. Commun. 49 (7) (2001) 1185–1191.

[35] C. Zhao, R.J. Baxley, Error vector magnitude analysis for OFDM systems, 2006 Fortieth Asilomar Conference on Signals, Systems and Computers, (2006), pp. 1830–1834.

[36] S. Park, B.W. Lee, S.H. Cho, Effect of the phase error, quadrature error, and i-q gain mismatch on symbol error probability for an M-PSK system in fading channels, 15th IEEE Intl. Symp. on Personal, Indoor and Mobile Radio Communications, PIMRC. 2 (2004), pp. 1317–1321, Vol. 2.

[37] G. Charalampopoulos, T. Dagiuklas, T. Chrysikos, V2I applications in highways: how RSU dimensioning can improve service delivery, Telecommunications (ICT), 2016 23rd International Conference on, IEEE, 2016, pp. 1–6.

[38] A. Yassin, Y. Nasser, M. Awad, A. Al-Dubai, R. Liu, C. Yuen, R. Raulefs, E. Aboutanios, Recent advances in indoor localization: A survey on theoretical approaches and applications, IEEE Commun. Surv. Tutor. 19 (2) (2017) 1327–1346, http://dx.doi.org/10.1109/COMST.2016.2632427

[39] S. Temel, M.C. Vuran, M.M.R. Lunar, R.K. Faller, C. Stolle, Vehicle-to-barrier communication during real-world vehicle crash tests, 2016 IEEE Vehicular Networking Conference (VNC), (2016), pp. 1–8.

[40] Alfa APA M25 dual band panel antenna datasheet, http://wlan-profi-shop.de/datasheet/APA-M25.pdf Accessed: 2017-04-30.

[41] Tp-link tl-ant5823b panel antenna datasheet, http://www.linkdataguard.com/datasheets/Wireless/TL-ANT5823B_V1_Datasheet.pdf Accessed: 2017-04-30.

[42] Air802 omni-directional antenna, https://www.air802.com/dual-band-mesh-wifi-omnidirectional-antenna-2.4-5.1-5.8-ghz-n-male.html Accessed: 2018-04-10.

[43] Example OFDM codes from GNU Radio, http://gnuradio.org/redmine/projects/gnuradio/repository/revisions/master/show/gr-digital/examples/ofdm

[44] Y. Shen, E. Martinez, Channel estimation in OFDM systems, 2006, (Freescale Semiconductor Application Note: AN3059).

[45] M. Haenggi, J.G. Andrews, F. Baccelli, O. Dousse, M. Franceschetti, Stochastic geometry and random graphs for the analysis and design of wireless networks, IEEE J. Sel. Areas Commun. 27 (7) (2009) 1029–1046.